SessionT3020

A high throughput screening approach to catalyst improvement for direct methanol fuel cell anodes

Kishori Deshpande[*], Alexander Mukasyan[*] and Arvind Varma[**]

---

[*] *Department of Chemical and Biomolecular Engineering,*
   Center for Molecularly Engineered Materials, University of Notre Dame
   Notre Dame, IN 46556

[**] *Author to whom correspondence should be addressed.*
School of Chemical Engineering, Purdue University, West Lafayette, IN 47907-2100
Tel: (765) 494-4075; Fax: (765) 494-0805; email: avarma@ecn.purdue.edu

Introduction

Liquid feed direct methanol fuel cells (DMFC) are promising candidates for portable power applications (1). The various cell components include Nafion electrolyte membrane, porous electrodes and bipolar plates. Platinum-based catalyst deposited on the porous electrodes helps to convert the fuel into benign by-products, H_2O and CO_2, along with generation of electricity. Currently, Pt-based catalysts are the only materials which exhibit high rates of methanol oxidation at fuel cell operating temperature (~ 80°C). However, platinum is not only expensive, but is also prone to poisoning due to the formation of intermediate organic species, such as carbon monoxide, during the process.

One promising approach to overcome these problems is to use nanoscale ***complex oxides*** (e.g. perovskites, cuprates, etc.) instead of conventional noble metal based ***anode catalysts*** in the DMFC. Note that this idea involves both complete and partial Pt/Ru replacement in the catalyst composition. In the latter case, it will also lead to reduction of Pt loading, which should be 0.2 mg/cm^2 or less to meet application needs (2). For example, high surface area perovskite electrocatalysts with the general composition ABO_3 (A=Sr, Ce, La, etc and B=Co, Fe, Ni, Pt, Ru, Pd etc) are attractive candidates for this application. The characteristic feature of these compounds is that there are numerous combinations of A and B cations that are possible. Substitutions on either or both sites offer the opportunity to manipulate the defect chemistry of the system. In particular, it is well documented (3) that cation substituents incorporated into the perovskite B-lattice have great influence upon overall electrocatalytic activity towards promoting a given electrochemical reaction. Thus, for efficient and systematic exploration of chemical "space" for signs of desired chemical activity one needs to employ: (a) *rapid method for synthesis* of such nanoscale materials with desired composition and purity; (b) *efficient screening technique*, which allows testing the materials for catalytic activities in conditions close to those in a fuel cell.

In the current work, we exploit the above-mentioned approach for screening the chemical space for catalytic activity. Specifically, in the first step, we use the aqueous combustion synthesis (CS) for rapid preparation of nanoscale materials. Details of this method can be found elsewhere [4-8]. In the second step, the catalytic activity of the obtained high surface area complex oxide powders is evaluated by using "High Throughput Screening Unit" - ***NuVant System***, which allows simultaneous comparison of catalytic activities for 25 different catalysts under DMFC conditions [9]. More specifically, the anode spots (0.71cm^2 each) are hot pressed with Nafion as an electrolyte and large surface area cathode (~100 cm^2) to prepare the membrane electrode assembly (MEA). Details of MEA preparation can be found in the experimental section. To measure the catalyst performance, methanol is fed at the anode with either hydrogen or air flowing on the cathode side. The current-voltage (I-V) curves generated for each composition are then compared with Pt-Ru standard for screening. Using this approach I-V performances of the prepared MEAs were investigated over a wide range of temperatures (60-90 ^{o}C), methanol flow (1-15 ml/min), and applied voltage scan rate.

Experimental Procedure

As mentioned earlier, the catalyst selection approach involved two steps: a) rapid synthesis of numerous compositions using the aqueous combustion synthesis, and b) rapid screening using the NuVant system. The experimental procedure for each step is explained separately next.

Step a: Rapid catalyst synthesis

A variety of compositions including $SmCoO_3$, La_2CuO_4 were synthesized in a chemical reactor made of quartz, which allows one to conduct experiments in different ambient atmospheres (i.e. air, oxygen, argon), measurements of temperature-time history of the reaction, and process monitoring by digital camera (Panasonic Digital Camcorder, Model PV-DV103). The temperature was measured using type K thermocouples (Omega Engineering Inc.) attached to multi-channel acquisition system (INET-200 controller card, Omega Engineering Inc) with rates from 5 to 60 samplings per second.

After reactants dissolution in sufficient amount of water (~15 ml) and thorough mixing of the obtained solution, the reactor was placed on a hot plate (Cole Parmer model 4803-00) and the mixture was preheated uniformly up to the water boiling point at rate ~5K/min (stage 1, Fig. 1). This was followed by relatively long (~5 min) constant temperature during which all free and partially bound water evaporated (stage 2, Fig. 1). The next preheating stage was characterized by higher rate (~12 K/min, stage 3, Fig. 1) and ended with either sudden (at some ignition temperature, T_{ig}) uniform temperature rise to a maximum value, T_m, or reaction initiated in a specific hot spot followed by steady wave propagation along the mixture (stage 4, Fig. 1). The rate of temperature change was high and in the range 10-10^4 K/s, with the duration of this high temperature region varying from ~10 to 100 seconds, and after cooling the synthesized products were typically fine solid powders.

The obtained products were analyzed for phase composition and crystallinity using X_1 Advanced diffraction system (Scintag Inc., USA). The powder microstructure was studied by field emission scanning electron microscopy (Hitachi, model S-4500) and the specific surface area was measured using BET analysis (Autosorb1C, Quantachrome Instruments).

Step b: Rapid catalyst screening

The catalytic performance of the synthesized powders was measured using the NuVant 1 system (Figure 2). As may be seen, hydrogen gas flow rate to cathode is accurately controlled using the mass flow controller before passing it through the humidifier bottles. Methanol is fed to the anode flow field using a peristaltic pump. The anode spots are connected to the data acquisition block though individual current collectors.

The screening involved numerous preparatory steps as discussed below. First, the powder samples, including standard Pt-Ru were dispersed in a suitable solvent such as methanol and iso-propanol and stirred to obtain the respective anode inks. The cathode consists of Pt-black catalyst and was prepared in a similar manner. Carbon paper (DeNora North America Inc., TGPH060 grade, non wet-proofed) is designed to maintain electrical contact and facilitate gas/fuel flow and thus functions as the gas diffusion layer. The total porosity of this substrate is too large (~80%) for optimum catalyst deposition. Hence to reduce it and increase its electronic conductivity, carbon ink prepared using the approach mentioned above, was applied with loading ~1 mg/cm^2. The respective catalyst inks were then applied to this support to obtain the anode and the cathode. The MEA was prepared by hot-pressing the electrodes with Nafion 117™ as an electrolyte at 160°C. Additional procedural details can be found elsewhere [10]. The I-V characteristics of the prepared MEAs were investigated under varying temperatures, scan and fuel flow rates.

Results

A: Rapid catalyst synthesis

A library of non-noble and partially substituted noble metal compositions was synthesized using the aqueous CS route. These included Fe_2O_3, $SmCoO_3$, Fe_3O_4, $CeFe_xNi_yO_3$ type systems. During the preparation, the effect of different reaction parameters such as type of fuel, ambient atmosphere, precursors on the final composition were also studied to explain the reaction mechanism. Details of these results can be found elsewhere [11].

B. Rapid catalyst screening

The synthesized compositions were tested for catalytic activity using the NuVant system. For better catalyst performance, in addition to high specific surface area of powders, it is important that the inks cover the surface uniformly. Hence, the anode disks were first characterized for surface coverage at different loadings using the SEM technique.

1: Optimization of catalyst loading

As seen in Figure 3, plain Toray Carbon paper was made from interwoven carbon strands about 7 μm thick. At higher magnification (Fig. 3b), the surface of each individual thread revealed wave-type heterogeneities ~ 30 nm in scale.

The SEM pictures of the carbon-ink treated carbon paper at different magnifications (Fig. 4) showed that the ink spread well over the paper, reducing the surface porosity (Fig. 4a). The microstructure of ink surface was not as smooth as the initial fibers (Fig. 4b) and average scale of heterogeneity was ~ 50 nm.

In the conventional case, the next step was deposition of Pt-Ru catalyst on the surface as shown in Figure 5a. To study the distribution of Pt-Ru catalyst on treated carbon paper, SEM pictures of the disk were taken in SEI and BEI modes. It can be seen (Fig. 5a), that the surface of the paper was essentially uniformly covered with the metal catalyst (light phase). The average size of Pt-Ru catalyst particle appeared to be 0.5μm (Fig. 5b).

One of the first oxide compositions for DMFC included $SmCoO_3$. Figure 6 indicates that under similar loading conditions as Pt-Ru, the surface was not uniformly covered with the catalyst (lighter phase), while average perovskite particle size was ~ 0.3μm (Fig. 5b). Based on these results, higher loadings of $SmCoO_3$ were used in NuVant trials as discussed below. Thus using this approach, loading optimization for various compositions was carried out.

2: Measurement of catalyst performance

Figure 7 shows typical I-V curves for standard Pt-Ru sample, where each curve corresponds to a specific Pt-Ru anode spot in the MEA. All curves show similar performance at the applied potential indicating the reproducibility of the results. Also, as expected, Pt-Ru shows kinetically controlled behavior at low voltages (~0.2V), while at higher voltages (~0.7V) it is mass transport limited and hence exhibits current saturation.

Of the different compounds tested for catalytic activity, Sr-based perovskites showed good performance as seen in Figures 8a and b. Further, trials conducted under different experimental conditions (temperatures, flow rates, duration of measurements, as well as different scan rates of applied voltage) confirmed that I-V curve for methanol decomposition on this perovskite surface has **complex non-monotonic** character (see Fig.8b). Qualitatively, the curve can be divided into **three regions**:
•   I – from 0.2 to ~0.32 V, where current increases with increasing applied voltage and reaches maximum at ~0.32 V. Note that in this region absolute current values obtained for perovskite catalysts are typically higher than those for Pt-Ru standard catalyst (see Fig. 8a).
•   II - ~0.35 – 0.8 V: current decreases and maintains relatively low (~0.005 A) values, thus indicating low catalytic activity of the catalyst (see Fig. 8b).
•   III – 0.8-1.4 V: current again increases to high absolute values (~0.2 A) and under some conditions, exceeds activity of the Pt-Ru standard catalyst (see Fig. 8b).

A comparison of activities for the standard Pt/Ru and Sr-based catalysts, in terms of the current values ratio as a function of applied voltage, is plotted in Figure 9. Since for DMFC the lower potential range (0-0.7V) is of interest, the figure concentrates on this regime. As reflected in the plot, in the range from 0 to 0.32 V, the current generated by reaction on the perovskite catalyst equals or is greater than that on standard Pt-Ru catalyst. However, owing to the effect of the current drop for the latter, in the voltage range 0.35-0.7 V, effectiveness of standard catalyst is higher (e.g. ~18 times at 0.7 V).

It was also shown that methanol flow rate in the range 1 –14 ml/min does not influence I-V characteristic of its decomposition on these catalyst (see Figure 10). These results indicate

that depletion of the fuel along the flow field is negligible, and that operation is in the kinetic regime for this composition.

Concluding Remarks

In the current work, a high throughput approach for synthesis and screening of catalysts for direct methanol fuel cell application was utilized. This method involved a) rapid synthesis of a library of compounds using the aqueous CS, and b) rapid screening using the high throughput NuVant system. First, by studying the surface coverage of catalyst inks under the SEM, we optimized its loading for uniform surface coverage and hence better activity. Second, a variety of powders were tested using the NuVant system and it was found that the Sr-based perovskites show comparable performance with Pt-Ru. This performance can be attributed to the high surface area and uniform phase composition obtained due to the advantages of combustion synthesis route viz., mixing on the molecular level and under the unique conditions of rapid high-temperature reactions. Thus, the method described here is a promising approach for catalyst screening for fuel cell applications.

Acknowledgement

References:

1. B. Gurau and E. S. Smotkin " Methanol Crossover in Direct Methanol Fuel Cells: A link Between Power and Energy Density", J. *Power Sources*, **112**, 339 (2002).

2. Larminie, J. and Dicks, A., *Fuel Cell Systems Explained*, John Wiley, Chichester, U.K. (2000).

3. White, J. and Sammels, F., "Perovskite Anode Electrocatalysis for Direct Methanol Fuel Cells", *J. Electrochem. Soc.*, **140**, 2167 (1993).

4. Deshpande, K. Mukasyan, A. and Varma, A. "Aqueous Combustion Synthesis of Strontium-Doped Lanthanum Chromite Ceramics" *J. Am. Ceram. Soc.*, **86**, 1149 (2003).

5. Patil, K.C.; Aruna, S.T.; Mimami, T. *Curr. Opin. Solid State Mater. Sci.* **2002**, *6*, 507.

6. Mathews, T. *Mater. Sci. Eng. B*, **2000**, *B78*, 39.

7. Rao, G. R.; Sahu, H. R.; Mishra, B.G. *Colloids Surf.*, *A*. **2003**, *220,* 261.

8. Fu, Y.P.; Lin, C.H. *J. Alloys Compd.* **2003**, *354*, 232.

9. Liu R., Smotkin E.S., "Array Membrane electrode assemblies for high throughput screening of direct methanol fuel cell anode catalysts", *J. Electroanal. Chem.* **535**, 49 (2002).

10. K. Deshpande, A. Mukasyan and A. Varma "A high throughput screening approach for DMFC anode catalyst selection", in preparation.

11. Deshpande, K., Mukasyan, A., Varma, A. "Direct Synthesis of Iron Oxide Nanopowders by Combustion Approach: Reaction Mechanism and Properties", *Chem. Mater*. In press.
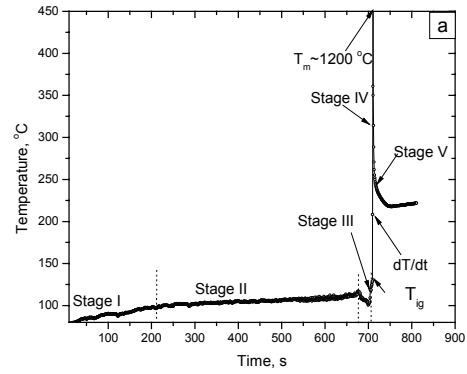
Figure1: Typical temperature-time profile during aqueous CS [11]
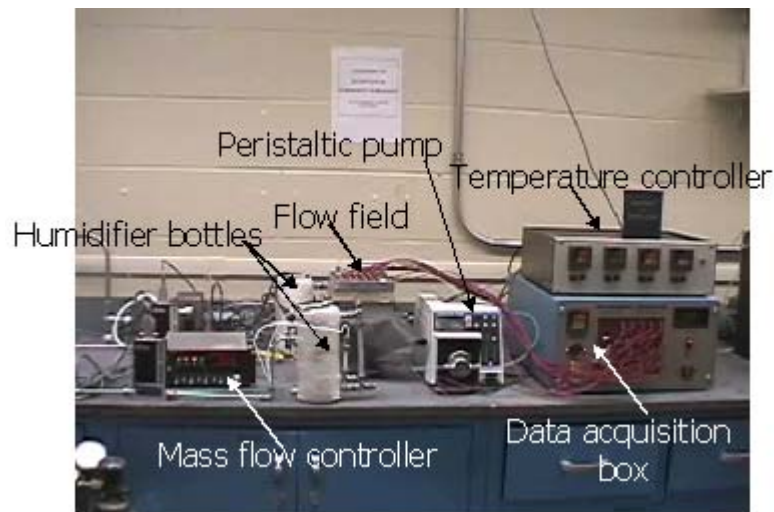
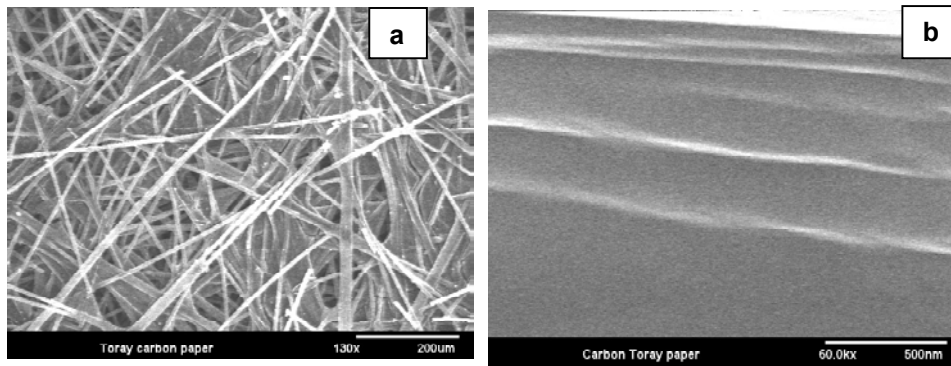

Figure 2: NuVant System with peripheral instruments

Figure 3: Secondary electron images of Carbon toray paper.
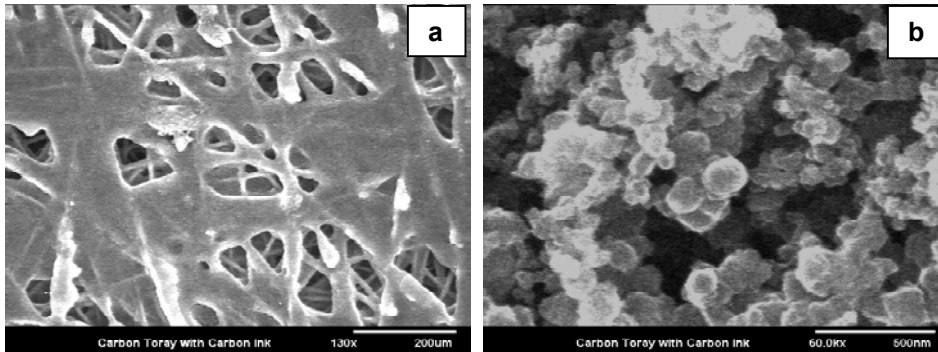
a) 130x b) 60Kx

Figure 4: Secondary electron images of carbon supported carbon toray paper
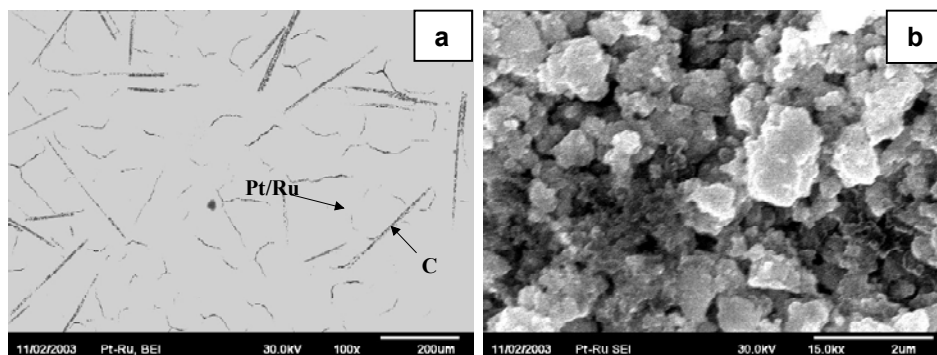
a) 130x b) 60Kx

Figure 5: Pt-Ru deposited on carbon supported toray paper
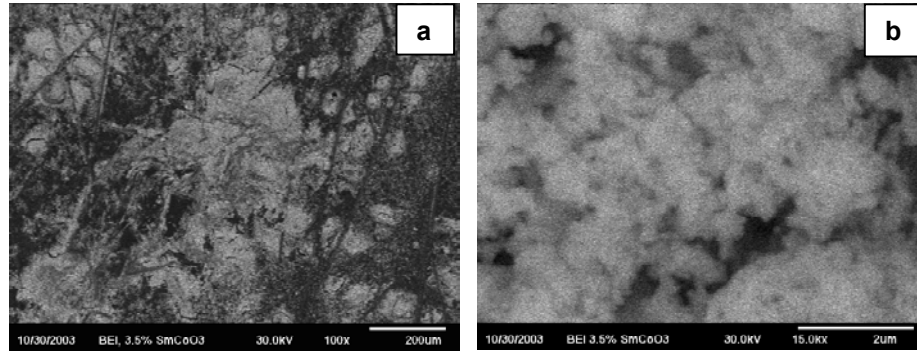
a) BEI 130x b) SEI 60Kx

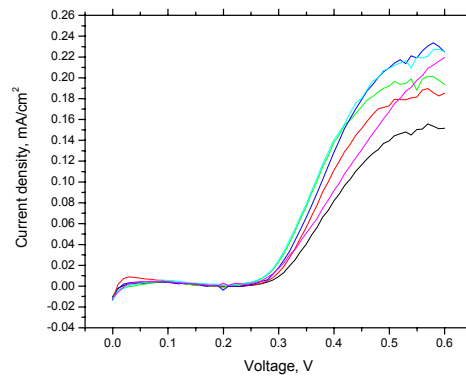Figure 6: SmCoO$_3$ deposited on carbon supported toray paper
a) BEI 130x b) SEI 60Kx
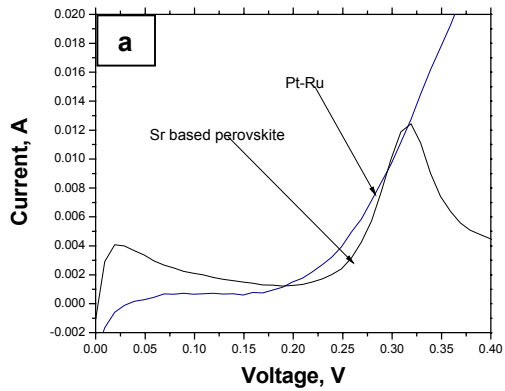

Figure 7: Typical I-V response for standard Pt-Ru sample
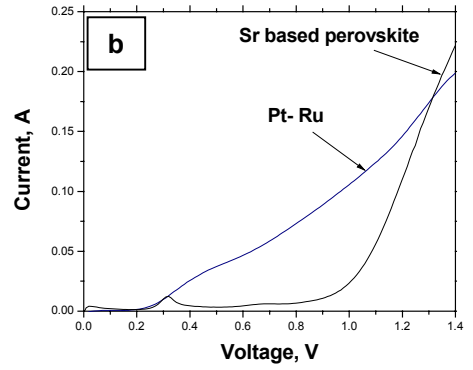
Figure 8: I-V response curves for Pt-Ru and Sr based perovskite in the range a) 0-0.4V b) 0-1.4V
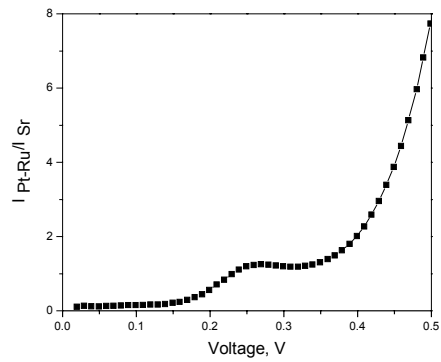

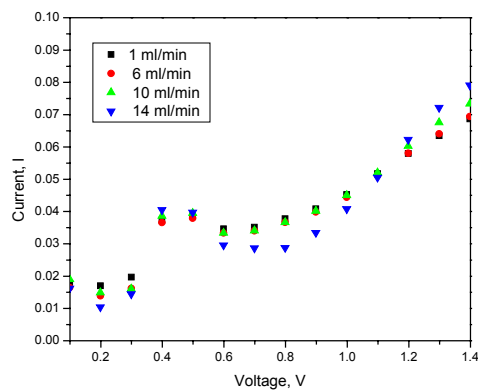Figure 9: Current ratio for Pt-Ru and Sr-based perovskite catalysts

Figure 10: Effect of flow rate on perovskite based catalyst performance